Photochemical & Photobiological Sciences

Accepted Manuscript

This article can be cited before page numbers have been issued, to do this please use: M. Penconi, M. Cazzaniga, S. Kesarkar, C. Baldoli, P. R. Mussini, D. Ceresoli and A. Bossi, *Photochem. Photobiol. Sci.*, 2018, DOI: 10.1039/C8PP00052B.

ROYAL SOCIETY OF CHEMISTRY

rsc.li/pps

View Article Online
DOI: 10.1039/C8PP00052B

Journal Name

ARTICLE

β-diketonate Ancillary Ligands in Heteroleptic Iridium Complexes: a balance between synthetic advantages and photophysical troubles

Received 00th January 20xx,
Accepted 00th January 20xx

DOI: 10.1039/x0xx00000x

www.rsc.org/

Marta Penconi[a§], Marco Cazzaniga[a§‡], Sagar Kesarkar[a§†], Clara Baldoli[a], Patrizia R. Mussini[b], Davide Ceresoli[a*] and Alberto Bossi[a*]

β-diketones are an important class of bidentate cyclometalating compounds, used in organometallic chemistry as ancillary ligands because of their wide commercial availability and the easy synthesis. They are employed to finely tune the electronic, spectroscopic and physical properties of metal complexes. Heteroleptic iridium complexes often advantage from the use of β-diketonates ligands, being their properties similar to those of the corresponding homoleptic tris-cyclometalated. Nevertheless, in some cases their use results in a complete quenching of the phosphorescence. Aiming to understand the origin of this drawback, we designed a suitable class of heteroleptic complexes and studied their thermal stability (DSC/TGA). We explored the effect of the ancillary ligand in a series of Ir(III) complexes bearing 2-phenylpyridine (*ppy*) as cyclometalated ligand and *acac* (acetylacetonate), *tta* (2-thienoyltrifluoroacetonate), *dtdk* (1,3-di(thiophen-2-yl)propane-1,3-dionate) and *BPhen* (4,7-Diphenyl-1,10-phenanthroline) as ancillary ligands. Through photochemical and electrochemical investigations, whose results agree and support our density functional theory calculations, we demonstrate that β-diketonate ligand with low triplet energy generates dark triplet excited states with negligible coupling to the ground state which indeed promote non-radiative relaxation through population of higher states.

Introduction

Tris-cyclometalated iridium complexes ($Ir(C^N)_3$, where C^N is a monoanionic ligand) have drawn great attention in the last decades, in particular due their excellent performances as phosphorescent emitters in optoelectronic applications, such as organic light emitting diodes (OLEDs).[1,2] In these complexes, the intense phosphorescence arises from a triplet ligand-centered (^{3}LC) excited state with the admixture of high-lying metal-to-ligand charge transfer state (MLCT). The strong spin-orbit coupling (SOC) induced by the iridium center favors the radiative emission from the triplet state to the singlet ground state, formally forbidden. Moreover, SOC promotes a high rate of intersystem crossing (ISC) from singlet excited states to the emitting triplet, thus allowing the harvesting of both singlet and triplet electro-generated excitons in OLEDs.
Fac-tris(2-phenylpyridinato-N^C2) Iridium(III) (**Ir3**) is the archetypal of the phosphorescent emitters for OLEDs, with impressive green emission efficiency, approaching unity. The frontier orbitals in **Ir3** are localized on the pyridyl π-orbitals in the LUMO, whereas the phenyl group and the iridium d-orbitals mostly contribute to the HOMO.[3] Hence, through careful engineering of a C^N ligand structure, the photophysical and electrochemical properties of the complex can be controlled to achieve emission from UV to near-IR.[4-6] The replacement of one of the C^N moieties with another cyclometalated "ancillary" ligand, yielding heteroleptic complexes with the optimal features of the homoleptic $Ir(C^N)_3$, provides the tool to fine control the color emission by selective stabilization/destabilization of the HOMO and LUMO levels. When chromophoric ancillary ligands are employed, additionally, the photophysics of the resulting molecule could be characterized by interligand energy transfer, in particular when the ligand triplets are close in energy.[7] Typical examples of ancillary ligands are β-diketone,[8] picolinic acid,[9] salicylimine[10,11] and pyrazolyl-borate[12] derivatives, to mention a few; among them, β-diketonate (O^O) ligands stand as the most popular and used. Many β-diketones are low cost, commercially available and the synthesis of the corresponding complexes is relatively easy. In addition, either their introduction produces no change in the luminescence color or they can induce a slight emission red-shift.[6,8] Functionalized 1,3-β-diketones have been widely used in lanthanide chemistry[13] and in recent years they demonstrated their potential as highly tunable conjugate scaffolds for the synthesis of luminescent materials.[14,15]

[a] *Istituto di Scienze e* Tecnologie Molecolari ISTM - CNR Via Golgi 19, 20133 Milano, PST via Fantoli 16/15, 20138 Milano and SmartMatLab Centre@ISTM, Via Golgi 19, 20133 Milano, Italy
* e-mails: davide.ceresoli@istm.cnr.it; alberto.bossi@istm.cnr.it
[b] Dipartimento di Chimica, Università degli Studi di Milano and SmartMatLab Centre, Via Golgi 19, 20133 Milano, Italy
‡ Currently Dipartimento di Chimica, Università degli Studi di Milano, Via Golgi 19, 20133 Milano, Italy
† Currently Departmento di Chimica, Università degli Studi di Bologna, Via Selmi 2, 40126 Bologna, Italy
§ Authors contribute equally to the work.
Electronic Supplementary Information (ESI) available: [Synthesis, thermal studies, electrochemistry, photophysics, DFT and TDDFT calculations]. See DOI: 10.1039/x0xx00000x

View Article Online
DOI: 10.1039/C8PP00052B

Journal Name

ARTICLE

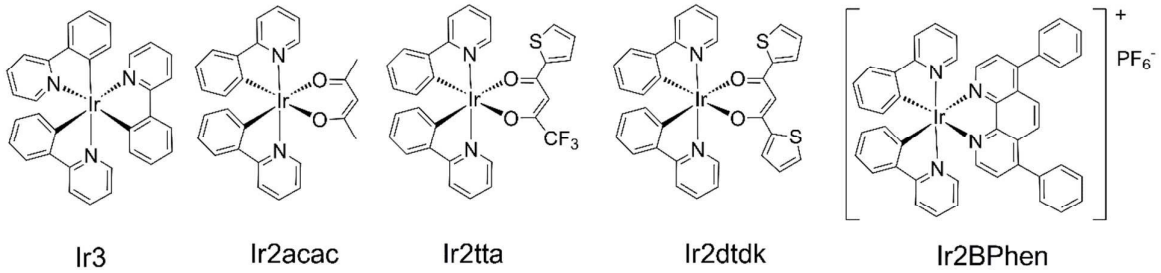

Chart 1. Chemical structures of the complexes.

In particular, upon coordination to B(III) Lewis acids like in diaroyl(methanato)boron difluoride systems, their photophysical behaviour have been investigated in both solution and solid state.[13,16,17] Acetylacetone (H*acac*) is the prototype of a non chromophoric β-diketonate ligand with the highest triplet energy.[18] Alkyl, fluoroalkyl, aromatic and/or heteroaromatic groups have been introduced as substituents on the carbonyl functions. All these functional groups affect different properties of the final β-diketonate complex; for instance, branched alkyl groups serve to enhance solubility and volatility, while aromatic substituents enhance light absorption but also influence the position of the energy levels of the ligand (*i.e.* singlet and triplet states). β-diketonates with heteroaromatic electron rich groups, such as thiophenes, were also proposed to be useful in certain optoelectronic applications, such as OLEDs, possibly enhancing the charge trapping ability of a complex or to provide sites (*e.g.* thiophene position) for a further modification.

In a recent work,[19] we compared a series of NIR emissive heteroleptic complexes having β-diketonate ancillary ligands with increasing conjugation: *acac*, *tta* (2-thienoyltrifluoroacetonate) and *dtdk* (1,3-di(thiophen-2-yl)propane-1,3-dionate). Although all the compounds have comparable photophysical and electrochemical properties, the phosphorescence efficiency was lower in the case of the *tta* derivative and that was attributed to a low-lying CT quenching state that can be thermally accessible from the lowest emissive state. Even worst could be the situation of some known compounds, like the $Ir(ppy)_2$dbm (*dbm*, 1,3-diphenylpropane-1,3-dione) where a complete quenching of the luminescence is observed.[8]

In this work we explore a series of complexes of formula $Ir(ppy)_2L$ (Chart 1) and carrying phenyl-pyridine (*ppy*) as the cyclometalated ligand, where L is a monoanionic or neutral bidentate ligand: *ppy*, giving the homoleptic **Ir3**; *acac*, *tta*, *dtdk* as β-diketonate ligands of different conjugation size giving **Ir2acac**, **Ir2tta** and **Ir2dtdk**, and *BPhen* (4,7-Diphenyl-1,10-phenanthroline) giving the cationic complex **Ir2BPhen**. *tta* and *dtdk* were selected according to their triplet energies compared to that of the *ppy* counterpart. We observed that the emission color and efficiency drastically change along this series: while **Ir3** and **Ir2acac** are highly efficient green emitters, a complete quenching of the emission occurs in **Ir2tta** and **Ir2dtdk**; **Ir2BPhen**, which exhibits optical and electronic features similar to the latter two complexes, displays a quite efficient orange emission. We will compare the electrochemical and optical properties of the complexes and, under the guidance of the theoretical modelling, we will address the origin of the quenched emission in *dtdk* and *tta* derivatives.

Results

Redox Properties

Electrochemical studies were performed to identify the nature and localization of the redox centers and gain informations on the frontier electronic levels of the complexes. Selected results, collected by cyclic voltammetry on a glassy carbon (GC) electrode in DMF solution with a 0.1 M TBAP supporting electrolyte, are reported in Table 1, while Figure 1 displays a synopsis of the CV patterns recorded at 0.1 V s^{-1}. The data of **Ir3** are taken from the literature and show reversibility both in the oxidation and reduction.[5] H*acac* and H*ppy* ligands have redox potentials that fall outside the solvent limits and thus would not be considered.

In all the β-diketonate complexes, a single, chemically and electrochemically reversible oxidation wave is detected above 0.4 V vs Fc^+/Fc. It is attributed, in analogy to previous data,[3,4] to a predominantly metal-centered process involving the cyclometalated phenyl-pyridine moiety,[20,21] as also evidenced by the DFT calculations. Similarly, to our previous study,[19] we observe a progressive shift of the complex oxidations (*i.e.* an HOMO level stabilization) towards more positive potentials following the order *acac* ≤ *dtdk* < *tta*. Although it should be considered that the negative charge on the tta^- and $dtdk^-$ could be stabilized by their larger π framework compared to the parent $acac^-$, thus resulting less available, the slight HOMO

View Article Online
DOI: 10.1039/C8PP00052B

stabilization (20 mV) occurring in the **Ir2dtdk**, compared to **Ir2acac,** could be more likely be attributed to the π-back-donation from the Ir(III) center to the *dtdk* ligand (again due to its extended conjugation).[22] Instead, the stronger positive shift (150 mV) of **Ir2tta** results from the combined effects of π-back-donation (in analogy with **Ir2dtdk**) and the electron-attracting effect of the CF_3 group on the *tta* moiety.

Ir2BPhen is the only ionic complex of the group. In this case, the oxidation potential undergoes a further positive shift accounting for the net positive charge centered on the iridium, that favors the π-donation from the N atoms of *BPhen* to Ir(III) while weakening the π-back-donation from the metal to *BPhen*. The complex oxidation, close to the solvent limit, is irreversible, although Dragonetti *et al.* reported the same process to be more reversible in acetonitrile solution and a return peak can be perceived increasing the scan rates.[21]

Within the solvent limits, no clear reduction waves are perceivable in the case of **Ir2acac** although a quite broad signal, on the solvent edge with onset around -2.28 V is observable. This would point to a peak close to -2.6 V as reported in previous works[8] and attributable to a one-electron reduction processes localized on the phenyl-pyridine ligand. **Ir2dtdk** and **Ir2tta** show a clear electrochemical and chemical reversible reduction at -2.16 and -1.99 V, respectively. The reduction cannot be reasonably attributed to a *ppy* based orbital (as in **Ir3** and **Ir2acac**) since the positive shift of 0.5 V cannot be explained with the effect of the ancillary ligand. Therefore, given that the free β-diketone are characterized by a reduction wave between -1.88 and -1.55 V (Table 1), the reduction process in **Ir2dtdk** and **Ir2tta** can be safely attributed to orbitals localized on the β-diketonate themselves. It is interesting to note that the reversibility is largely improved compared to the free ligands[23] and that upon coordination to the iridium center the reduction potential of *dtdk* undergoes a smaller negative shift (0.32 V) compared to the 0.48 V observed in *tta*. The different shifts provide a further inside on the donation and back-donation processes and kindly match with the interpretation that *tta* ligand favors a stronger back donation from the metal center.

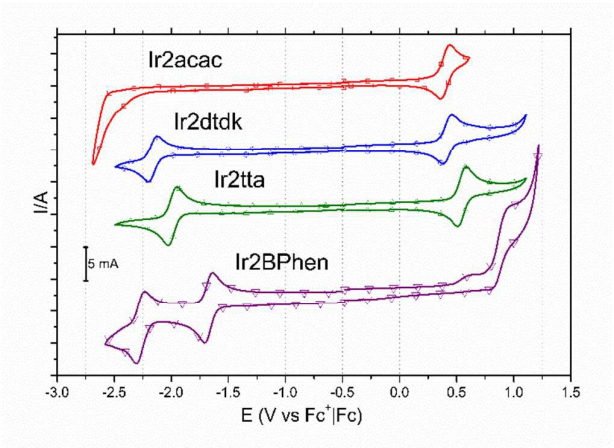

Figure 1. Cyclic voltammograms of the complexes recorded versus Fc^+/Fc in DMF at 298 K under a N_2 atmosphere (scan rate = 100 mV s^{-1}).

Finally, **Ir2BPhen** displays two clear reversible reductions at -1.67 and -2.27 V vs $Fc^+|Fc$. The less negative process is ascribed to orbitals localized onto the *BPhen* ligand as already discussed in the literature;[21] the second reductive event is presently difficult to assign. In fact, the uncoordinated *BPhen* ligand is characterized by two *quasi*-reversible and nearly merging reductions (see Fig. SI8).[24] Once it is cyclometalated to iridium, it acts as neutral N donor compound, therefore its electron poor character allows for easier reduction compared to the uncoordinated system. Hence, a one electron reduction in **Ir2BPhen** removes the degeneracy. Therefore, the peak at -2.27 V may belong either to a second reduction on the ancillary *BPhen* ligand or it can be ascribed to a *ppy* based process (considering that, being the oxidation at 0.93 V, this potential is consistent with an optical band gap of 2.5 eV).

DFT/TDDFT Calculations

The molecular orbitals (MOs) obtained at the DFT-B3LYP level are reported in Figures 2 and SI9. The visual inspection shows that the HOMO are localized mainly on the *ppy* moiety. The LUMO of **Ir3** and **Ir2acac** are also localized on the *ppy*, whereas the LUMO of **Ir2dtdk** and **Ir2tta** are on the ancillary ligand, with a modest contribution from the metal d-states. Interestingly, **Ir2BPhen** has a two-fold degenerate LUMO, localized on the *BPhen* moiety. Once, the LUMO get occupied by one electron, the degeneracy is lifted because of Coulomb repulsion and the once-degenerate companion MO, is pushed higher in energy.

Table 1. Electrochemical data of the complexes.

	E_{ox} [E_{ox}^o] (V)	$E_{ox\ onset}$ (V)	E_{red} [E_{red}^o] (V)	$E_{red,onset}$ (V)	$E_g^{\ o}{}_{max}$ (eV)	$E_{g,onset}$ (eV)	HOMO (eV)	LUMO (eV)
Ir3[5]	//	+0.31	//	-2.70	//	3.01	-5.11	-2.10
Ir2acac	+0.43[r] [+0.40]	+0.32	//	-2.28	//	2.60	-5.12	-2.52
Ir2dtdk	+0.46[r] [+0.42]	+0.35	-2.20[r] [-2.16]	-2.09	2.58	2.44	-5.15	-2.71
Ir2tta	+0.58[r] [+0.55]	+0.47	-2.03[r] [-1.99]	-1.92	2.54	2.39	-5.27	-2.88
Ir2BPhen	+0.93[i]	+0.75	-1.70[r] [-1.67], -2.30[r] [-2.27]	-1.60	2.63	2.35	-5.55	-3.20
Hdtdk	+1.06[i]	+0.85	-1.88[q], -2.17[q]	-1.73	//	2.58	-5.65	-3.07
Htta	//	+1.04	-1.55[i], -2.09[i]	-1.41	//	2.45	-5.84	-3.39
BPhen	//	//	*-2.40*[q], *-2.53*[q]	*-2.17*	//	//	//	*-2.63*

$E^o=1/2(E_{pa}+E_{pc})$; DMF/TBAP (0.1 M), vs $Fc^+|Fc$ at scan rate 100 mVs^{-1}; [r] denotes reversible; [i] denotes irreversible and [q] denotes quasi-reversible peaks. $E_g^{\ o}{}_{,max} = (E_{ox}^o - E_{red}^o)$. $E_{g,onset} = (E_{ox,onset} - E_{red,onset})$. The HOMO energy level was calculated using the equation E_{HOMO} (eV) = -($E_{ox\ onset}$ + 4.8) and LUMO energy level was calculated using the equation E_{LUMO} (eV)= -($E_{red,onset}$ +4.8). The bandgap was determined from the equation E_g (eV)= -(E_{HOMO}– E_{LUMO}). The onset potentials of oxidation and reduction are determined from intersection of the tangents drawn at the rising current side of the peak and the extrapolated baseline charging current of the CV.

View Article Online
DOI: 10.1039/C8PP00052B

Journal Name

ARTICLE

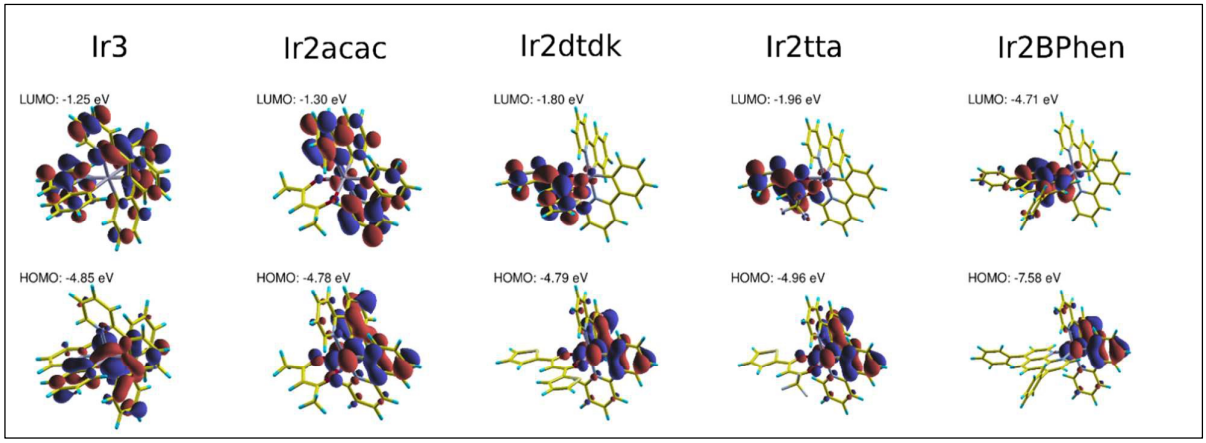

Figure 2. Frontier molecular orbitals calculated at the B3LYP level.

Note that we did not include a compensating anion in the calculation of **Ir2BPhen** and, because of the net charge, all MO energy levels are lower in energy with respect to the others systems. Thus, excluding **Ir2BPhen**, the energy of the HOMOs and of the LUMOs correlate fairly well with the oxidation and reduction peaks of the CV experiments.

It should be noted however, that the molecular orbital energies are an approximation to the CV oxidation/reduction levels.[25] If the Koopman's condition would be fulfilled exactly by the exchange-correlation potentials, and in absence of orbital relaxation, they two would correspond exactly. It has been shown that hybrid-XC functional can fulfil the Koopman's condition quite well. The total energy as a function of the number of electrons is nearly piece-wise linear (the small deviation from linearity is the Hubbard energy, i.e. the charging/discharging energy in CV). This Hubbard energy is due to the residual electron self-interaction and is of different magnitude between occupied (HOMO) and unoccupied (LUMO) states.[26]

The calculated absorption spectra, at the TDDFT-B3LYP level, are reported in Figure SI11 and in Tables from SI2 to SI11. The energy of the transitions and their oscillator strength are in overall good agreement with the experimental spectra.

Table 2. Calculated phosphorescence emission energies.

	ΔSCF(0-0)	ΔSCF(vertical)	TDA
Ir3	2.5262 eV (486.9 nm)	2.2714 eV (545.8 nm)	2.2580 eV (549.1 nm)
Ir2acac	2.4378 eV (508.6 nm)	2.2500 eV (551.0 nm)	2.1700 eV (571.3 nm)
Ir2dtdk	2.0545 eV (603.5 nm)	1.6178 eV (766.4 nm)	1.4290 eV (867.6 nm)
Ir2tta	2.0285 eV (611.2 nm)	1.4802 eV (837.6 nm)	1.2981 eV (955.1 nm)
Ir2BPhen	2.3438 eV (552.6 nm)	2.0953 eV (591.7 nm)	1.7459 eV (710.1 nm)

In Table 2 we report the calculated emission wavelengths, according to three different methods. As shown in previous publications,[19,27] the ΔSCF method slightly overestimates the wavelength in these systems, but is more accurate than TDDFT (in the Tamm-Dancoff Approximation). As the emission shape is temperature dependent in experiments, the ΔSCF(0-0) and ΔSCF(vert.) results provide in practice, upper and lower bounds for the emission. This is true for **Ir3**, **Ir2acac** and **Ir2BPhen**. However, the calculated emission wavelength of **Ir2dtdk** and **Ir2tta** strongly overestimates the experimental emission peak. This could mean that either the lowest T1 is not emissive, or emission arises from a different state, competitive with T1.

Photophysical Properties

The absorption spectra of the complexes in CH_2Cl_2 are reported in Figure 3. All the compounds show intense bands below 320 nm, with absorptivity exceeding $2.5x10^4$ L mol^{-1} cm^{-1} (Table 3). While **Ir3** displays two distinct peaks at 243 nm and 282 nm, in the heteroleptic complexes the transition slightly red-shifts along the series: **Ir2acac** (260 nm), **Ir2tta** (266 nm), **Ir2dtdk** (268 nm) and **Ir2BPhen** (272 nm). These bands in the UV region match the free ligand absorptions (See Figure SI 6 in ESI) and are attributed to the spin allowed π-π* transition (^{1}LC) of the organic moieties. In all the complexes, the weaker absorption at lower energy (320 - 440 nm, ε < 23000 L mol^{-1} cm^{-1}) accounts primarily for the spin allowed d–π* transition (^{1}MLCT states), although contributions from ^{1}LC states of the β-diketonate ancillary ligands are present in this spectral region for **Ir2tta** and **Ir2dtdk**. Finally, the broad and unstructured absorption, in the range 440 - 550 nm, with extinction coefficient below 4000 L mol^{-1} cm^{-1}, accounts for

View Article Online
DOI: 10.1039/C8PP00052B

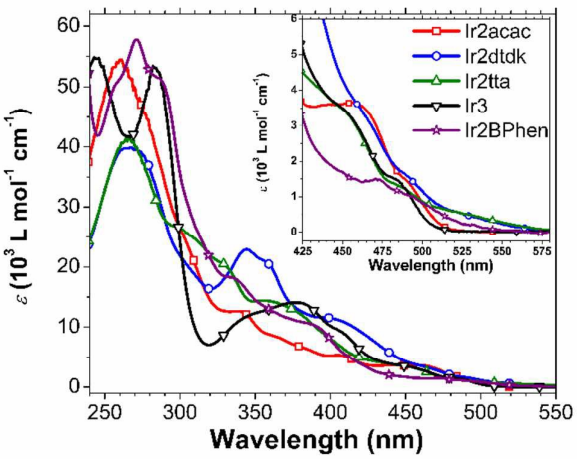

Figure 3. UV/Vis absorption spectra in CH_2Cl_2 at 298 K of complexes **Ir3** (black inverted triangles), **Ir2acac** (red squares), **Ir2tta** (green triangles), **Ir2dtdk** (blue circles) and **Ir2BPhen** (purple stars). S0–T1 absorption bands in the inset.

transitions of triplet character. Overall, giving attention to the absorption onset there is a progressive shift towards low energies on going from **Ir3** > **Ir2acac** > **Ir2Bphen** and **Ir2tta** ≈ **Ir2dtdk**

Photoluminescence experiments were performed in degassed solution of CH_2Cl_2 at room temperature and in glassy matrix of 2-MeTHF at 77 K (Figures 4 and SI7, Tables 3 and SI1). **Ir3** and **Ir2acac** have been already extensively studied. Both are known to be highly phosphorescent green emitters (from a predominant ^{3}MLCT state involving the occupied Ir-5d and unoccupied *ppy* π^* orbitals).[3] At room temperature the two complexes emit at 515 nm and 520 nm, respectively, (Figure 3) with phosphorescence quantum yield and lifetime of 95% and 1.5 µs for **Ir3**, 62% and 1.6 µs for **Ir2acac.**The heteroleptic structure of the **Ir2acac** and the different geometric orientation of the *ppy* ligands (Chart 1) result in an increase of k_{nr} by one order of magnitude with respect to the homoleptic complex. The modification of the β-diketonate ligand by the introduction of one thiophene ring and one electron-drawing CF_3 group, as in **Ir2tta,** or the by bis-substitution with thiophenes, as in **Ir2dtdk**, result in an almost completely quenched room temperature phosphorescence (QY < 0.01). The emission maintains the unresolved broad feature of the parent **Ir2acac** complex although slightly blue shifted at 519 nm and 515 nm for **Ir2tta** and **Ir2dtdk**, respectively. Despite the low QY, the excited state lifetimes are barely reduced compared to **Ir2acac**, being 1.3 µs and 1.5 µs, respectively.

The spectral features suggest that the two complexes still emit from a ^{3}MLCT state centered on *ppy* ligand, although radiative rates (k_r = 7-8x10^3 s^{-1}) are two order of magnitude smaller than that of **Ir2acac,** while k_{nr} constants only slightly increase.

The cationic complex **Ir2BPhen** has a complete different behavior with emission maximum at 588 nm, quantum yield of 77% and a lifetime of 1.1 µs. It is considerably red-shifted with respect to all the other complexes. In agreement with the reported literature, its emission can be assigned to a ^{3}MLLCT (metal-ligand-to-ligand-charge transfer) emitting state from the *ppy* ligand to the *BPhen* one. The broad band (FWHM = 3100 cm^{-1}) and the large Stokes shift confirm a greater spatial separation of the involved states.

In glassy matrix at 77 K, **Ir3** and **Ir2acac** exhibit a well resolved vibronic structure with maxima at 494 and 506 nm, respectively. The emission blue-shift with respect to room temperature, i.e. rigidochromic effect, accounts for 825 and 532 cm^{-1}, respectively. This effect is due the stabilization of the emitting state upon solvent reorganization at room temperature, whereas it is hampered in rigid matrix at 77 K, and it is directly related to the degree charge redistribution between excited and ground states.[19] Complex **Ir2BPhen** is quite emblematic since it undergoes over 2400 cm^{-1} emission blue-shift at 77 K with a complete change in spectral shape becoming structured and equivalent to a *ppy* based process.

At low temperature **Ir2dtdk** and **Ir2tta**, still show very low emission intensity with peculiar behaviors. Both complexes display instead a new broad and unstructured low energy band at around 630 nm with microsecond decay regime. Moreover, **Ir2tta** displays a residual high energy emission at 497 nm, absent in the case of **Ir2dtdk**.

Discussion

All complexes were synthesised in good overall yields by means of standard procedures as described in the ESI.

The iridium complexes can be used as emitters in a simple multi-layer OLED architecture (+)ITO/HTL/EML/ETL/LIF/Al(-), where HTL (hole transport layer) could be 4,4'-bis[N-(naphthyl)-N-phenyl-amino]biphenyl (NPD), ETL (electron transport layer) could be 2,9-dimethyl-4,7-diphenyl-1,10-phenanthroline (BCP) and the EML (emitting layer) could be a blend of the iridium complex doped into a host matrix.

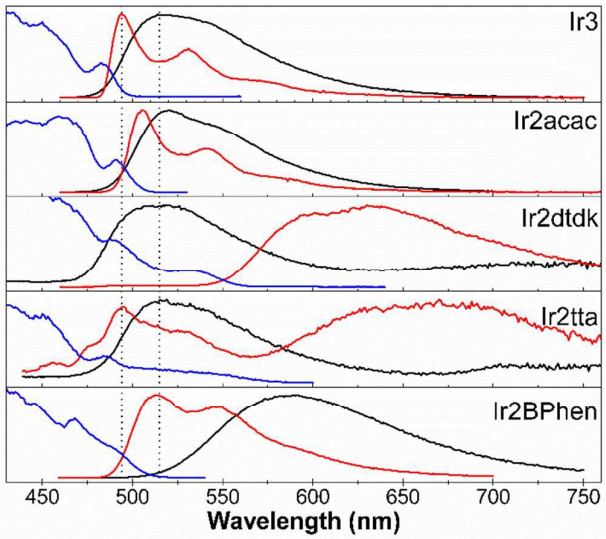

Figure 4. Normalized emission spectra in degassed CH_2Cl_2 solution at 298 K (black line); excitation (blue line) and emission (red line) spectra in glassy 2-MeTHF at 77 K, for the complexes.

View Article Online
DOI: 10.1039/C8PP00052B

Journal Name

ARTICLE

Table 3. Photophysical data of the complexes.

	λ_{abs} (nm) ($\varepsilon(10^3$ L mol^{-1} cm^{-1}))[a]	298 K[b]					77 K[c]	
		λ_{em} (nm)	τ (µs)	Φ_L	k_r (10^5 s^{-1})	k_{nr} (10^5 s^{-1})	λ_{em} (nm)	τ (µs)
Ir3	243 (54.8), 282 (53.4), 340 [sh] (11.1), 378 (14.1), 405 (9.52), 455 (3.26), 485(1.45)	515	1.5	0.95	6.17	0.325	494	4.5
Ir2acac	260 (54.5), 306 (23.0) [sh], 338 (12.6), 366 (8.16), 405 (5.26), 457 (457), 492 (1.33)	520	1.6	0.62	3.76	2.30	506	5.0
Ir2dtdk	268 (39.8), 344 (22.8), 358 (20.7) [sh], 401 (11.4), 465 (3.16)	515	1.5	*< 0.01*	*≈0.066*	*≈6.6*	600, 630	-
Ir2tta	266 (41.7), 303 (26.0), 331 (20.0), 363 (14.1), 450 (3.47)	519	1.3	*< 0.01*	*≈0.077*	*≈7.5*	493, 645	-
Ir2BPhen	272 (57.7), 288 (51.0), 338 (17.9), 391 (10.2), 472 (1.55)	588	1.1	0.77	6.91	2.02	513	5.7

[a] Absorption maxima and molar extinction coefficients in CH_2Cl_2 at 298 K. [b] Phosphorescence maxima, lifetimes and quantum yields in degassed CH_2Cl_2 at 298 K. Radiative and non-radiative rate constants are calculated using the equations $k_r = \Phi_L/\tau$ and $k_{nr} = 1/\tau - k_r$, on the assumption $\Phi_{ISC} = 1$. [c] Phosphorescence maxima and lifetimes in 2-MeTHF at 77 K. k_r and k_{nr} for **Ir2tta** and **Ir2dtdk** are indicative given the too large variability in accessing Φ_L.

By considering both the energy of the frontier levels and triplet states of the dopant, 4,4'-N,N'-dicarbazol-biphenyl (CBP) could be suitable as host material since its HOMO/LUMO levels comprise the ones of the emitters, thus allowing for an efficient charge trapping. Moreover, the CBP triplet energy is higher than the those of the emitters, as necessary to guarantee the triplet harvesting.[28] The requirements are fulfilled for all the investigated compounds, despite the negligible emitting efficiencies of **Ir2dtdk** and **Ir2tta** make them not suitable as OLED emitters.

In order to assess the possible use of these compounds as guest emitters in vacuum deposited OLEDs, thermal studies were performed by DSC and TGA methods, under nitrogen atmosphere. Good stability is found for all the complexes, except **Ir2BPhen** that is the only one showing an exothermic degradation process. **Ir3** results as the most stable compound up to 444°C (melting, T_m) with less than 5-8 % weight loss (*w.l.*) below 350°C; **Ir2acac** shows T_m=330°C with less than 5% *w.l.* below 290°C; **Ir2tta** shares similar stability as **Ir2acac** with T_m=327°C and less than 5% *w.l.* below 325°C. The new **Ir2dtdk** shows improved stability with T_m= 355°C and less than 5% *w.l.* below 345°C. The cationic complex **Ir2BPhen** instead displays an exothermic decomposition process starting at ca. 320°C.

Analysing the frontier electronic levels of the iridium complexes and their ligands from both the DFT calculations and the electrochemical studies (in full agreement), it is evident that in all the complexes the HOMO level is characterized by a strong contribution from the metal center and the cyclometalated phenyl group of *ppy* ligand. HOMOs experience a progressive energy stabilization in the sequence *acac*, *dtdk*, *tta*; **Ir2Bphen** stands slightly out of this series simply for its formal cationic nature leading to over 0.4 eV shift of the HOMO down in energy compared to the other complexes. The observed irreversibility might be related to the experimental conditions (reversibility is restored at high scan rate) since previous investigations indicate the oxidation of **Ir2Bphen** reversible.[21] The LUMO levels in **Ir3** and **Ir2acac**, as widely discussed in the literature, are localized on the cyclometalated C^N ligand and mainly on the pyridine portion. Contrary, in the other systems, the LUMO level shifts onto the ancillary ligands (either the β-diketonate or the phenanthroline one). DFT investigation safely confirms this picture and indicates that the LUMOs+1 are localized on *ppy* moiety. **Ir2BPhen** displays an interesting behaviour: similar to the free *BPhen* ligand, it has two nearly degenerate levels, while the LUMO+2 shows a *ppy* character, although this situation may change upon one electron reduction (*ppy* on LUMO+1). In **Ir2BPhen**, upon cyclometalation of *BPhen*, its LUMO drops in energy (with respect to free *BPhen*) accounting for the π-bonding to the Ir center; the two complexes **Ir2tta** and **Ir2dtdk**, display a reverse behaviour since first reduction occurs at more negative potentials compared to the free ligands.

Considering the absorption spectra of the free ligands (see Figure SI6), their singlet excited state energy decreases along the series H*ppy*≈H*acac*>*BPhen*>H*tta*>H*dtdk*. Taken from low temperature measurements, their triplet energy ranks H*acac* as the higher T state at 3.14 eV, followed by the triplet of H*ppy* (2.88 eV),[29] Ir(ppy)$_2$ fragments (2.51 eV), *BPhen* (2.48 eV),[30] H*tta* (2.47 eV)[31] and H*dtd*k (2.33 eV)[31].

Calculations highlight that the transition to the S1 state is optically inactive in all systems except for **Ir3** and **Ir2acac** and

View Article Online
DOI: 10.1039/C8PP00052B

in fact no feature of their MLLCT transition into the ancillary ligand are evident in the absorption spectra (UV-Vis shows spectra rather similar one to the other); in turn excitation spectra at 77K reveals long-wavelength signal in the case of **Ir2tta** and **Ir2dtdk** with offset around 585 and 570 nm and 520 nm for **Ir2BPhen**). Moreover, the corresponding T1 state, localized on the ancillary ligand, has a non-emissive character in the case of **Ir2tta** and **Ir2dtdk**; their weak phosphorescence at low energy is observed only at 77 K. TDDFT calculation predicts a triplet emission energy for **Ir2tta** and **Ir2dtdk** in good agreement with their red phosphorescence at 77 K, although the green emission at 298 K is not explained.

In order to give an explanation of the emission in **Ir2dtdk** and **Ir2tta**, we extracted the Mulliken spin density on the Ir ion in the T1 state (Table SI12) and we examined the changes of the geometry between the S0 and the lowest T1 state (Table SI13). The spin density shows that the metal d-states contributes nearly the same in all heteroleptic compounds. This contribution is slightly smaller in **Ir2dtdk**, with respect to the other four molecules. In **Ir3**, there is charge donation from the ligands into the minority spin channel of the Ir ion, and as a consequence its spin density is reduced. Our findings point towards the fact that spin orbit (SO) effects are of the same magnitude in all the compounds and do not explain the difference in the phosphorescence colors.

Next, we extracted from our DFT calculations, the distance between Ir and its neighboring atoms, in the S0 and T1 states. Interestingly, we found that on going from the S0 to the T1 there is an average contraction of the first shell of atoms surrounding the metal. On average, this contraction is quite small (−0.005 Å) for **Ir3** and **Ir2acac**, and larger (−0.021, −0.025 Å) for **Ir2dtdk** and **Ir2tta**, respectively. The case of **Ir2BPhen** is intermediate, with an average contraction of −0.015 Å. A large geometrical rearrangement reflects a large difference between the S0 and the T1 potential energy surfaces (PES). As a result, in **Ir2dtdk** and **Ir2tta**, non-radiative processes might dominate over the photoemission from the lowest triplet state.

Therefore, our DFT and TDDFT results suggest the following scenarios: the lowest singlet of **Ir2dtdk** and **Ir2tta** is of MLLCT character with a very small oscillator strength. Moreover, the singlet- triplet splitting is very small (~0.03 eV) and comparable with thermal energy at room temperature. Considering that the T1 state is not well vibronically coupled to the ground state, it is conceivable that the triplet is depopulated in favor of other higher T states by reverse internal conversion (rIC) or S states by reverse ISC; states which in turn emits to the S0, suggesting a possible thermally activated process (TAP).

On the contrary, the singlet-triplet splitting of **Ir3** and **Ir2acac** is one order of magnitude larger and these compounds show conventional phosphorescence. The case of **Ir2BPhen** is intermediate and, since the *BPhen* moiety is more rigid, it is conceivable that the T1 could have two competing pathways for emission: via vibronic coupling to the S0 and by TAP.

Conclusion

β-diketonate ancillary ligands are used in the chemistry of heteroleptic iridium complexes as a tool to finely tune the electronic, spectroscopic and physical properties of the resulting compounds. Nevertheless, in some cases their introduction may ultimately lead to a partial or complete quench of the emission. For this reason, we investigated a series of heteroleptic complexes carrying β-diketonate ancillary ligands with progressively lower triplet energy. By studying their electrochemical behavior, we determined the nature and localization of the frontier energy revealing that although the HOMO energy is sensitive to the ancillary ligands structure, it always locates on the Ir center and the phenyl group of *ppy*. On the contrary, the LUMO level shifts from the *ppy* ligand to the ancillary one in those complexes with quenched emission. Photophysics reveals a quite peculiar emissive behavior with a strong color change between room temperature and 77 K. Spectroscopy, matched to the electrochemical studies, agrees and grants support to the theoretical framework developed. TDDFT calculations revealed a complex situation when the β-diketonate ligand represent the lowest triplet state of the complex. The corresponding HOMO-LUMO transition from the ground state has negligible oscillator strength because of the poor wavefunction overlap. Moreover, the strong charge transfer character of the transition shrinks the singlet-triplet splitting to the order of the thermal energy at 298 K, promoting the back energy transfer to the higher states, as the main deactivation channel for the non-emissive triplet. This phenomenon looks to be more general than the example herein described and applies also to literature cases,[7,32,33,34,35] and it should be considered in the situation where one of the frontier orbital (*i.e.* LUMO), fully shifts onto the ancillary ligand.

Experimental

Reagents and solvents were purchased from Aldrich and TCI and used without further purification. All solvents, unless otherwise stated are degassed under argon prior the use. The ligand H*dtdk* was previously synthesized by some of us,[31] while H*tta* and H*dpm,* commercially available, were used as received. NMR were recorded on Bruker Advance 400 MHz and the residual signal of the deuterated solvent was used as internal standard (e.g. 5.32 ppm for ^{1}H and 53.84 ppm for ^{13}C of CD_2Cl_2). The chemical shifts are given in ppm and coupling constants in Hz. **Ir3**[36], **Ir2acac**[37], **Ir2tta**[23] and **Ir2BPhen**PF_6[21] were synthesized according to known synthetic procedures.

Ir2dtdk was synthesized in this work and details are given in Supporting Information.

Complex **Ir2dtdk**: (400 MHz, CD_2Cl_2) δ = 8.62 (d, *J*=5.8 Hz, 2H), 7.90 (d, *J*=8.1Hz, 2H), 7.75 (t, *J*=7.9Hz, 2H), 7.62 (d, *J*=7.8Hz, 2H), 7.60 (d, J=3.8Hz, 2H), 7.43 (d, *J*=4.7Hz, 2H), 7.13 (t, *J*=7.8Hz, 2H), 7.02 (dd, *J*=4.7Hz, 1H), 7.01 (d, *J*=3.8Hz, 1H), 6.88 (t, *J*=7.4Hz, 2H), 6.74 (t, *J*=7.4, 2H), 6.47 (s, 1H), 6.29 (t, *J*=7.6Hz, 2H).

View Article Online
DOI: 10.1039/C8PP00052B

^{13}C-NMR (100 MHz, CD_2Cl_2) δ = 172.9, 168.1, 147.7, 147.4, 145.7 (Cq), 148.8, 137.9, 133.6, 129.8, 129.4, 128.5, 127.6, 124.4, 122.5, 121.4, 119.1, 94.5 (CH)
LC-MS= 735.8 $[M]^+$, M^2 (735.8) = 500.9 $[M\text{-}dtdk]^+$
Anal. Calc. for $C_{33}H_{23}IrN_2O_2S_2$: C, 53.86; H, 3.15; Ir, 26.12; N, 3.81; O, 4.35; S, 8.71; Found: C, 53.05; H, 3.3; N, 3.63.

Electrochemical measurements were performed using potentiostat-galvanostat AUTOLAB PGSTAT of EcoChemie (Utrecht, The Netherlands), equipped with software GPES version 4.9 for the processing of experimental data. Cyclic voltammetry patterns were recorded on a wide range of scan rates on a glassy carbon (GC) working electrode (Metrohm, 3 mm diameter), using a platinum counter electrode and an aqueous saturated calomel electrode (SCE) inserted in a separated compartment filled with the working medium and ending with a porous frit to avoid significant leakage of water and chloride anions. The experiments were carried out in dimethylformamide (DMF) at $3x10^{-3}$ M concentration of the complex in the presence of tetrabutylammonium perchlorate salt (0.1 M) as supporting electrolyte, removing oxygen by nitrogen bubbling. The potentials were subsequently referred to the potential of the Fc^+/Fc couple recorded in the same conditions. Ohmic drop correction was applied by the positive feedback method.
UV/Vis absorption spectra were obtained on Agilent 8453 spectrophotometer in 1 cm path length quartz cell in $2x10^{-5}$ M CH_2Cl_2 solution. Photoluminescence quantum yields were measured with a C11347 Quantaurus - QY Absolute Photoluminescence Quantum Yield Spectrometer (Hamamatsu Photonics U.K), equipped with a 150 W Xenon lamp, an integrating sphere and a multi-channel detector.
Steady state emission and excitation spectra and photoluminescence lifetimes were obtained with a FLS 980 spectrofluorimeter (Edinburgh Instrument Ltd.). Continuous excitation for the steady state measurements was provided by a 450 W Xenon arc lamp. Photoluminescence lifetime measurements, determined by TCSPC (time-correlated single-photon counting) method, were performed using an Edinburgh Picosecond Pulsed Diode Lasers EPL-445 and EPL-375 (Edinburgh Instrument Ltd.), with central wavelength 442.2 nm and 374.0 respectively, repetition rates 50 μs or 20 μs. Photoluminescence experiments at room temperature were carried out in nitrogen degassed $2x10^{-5}$ M CH_2Cl_2 solution. Measurements at 77 K were performed in 2-MeTHF frozen matrix.
DSC were measured in open vessel mode under nitrogen flow on a Mettler Toledo STARe SYSTEM DSC 500 and TGA analysis were performed under dry nitrogen flow on a Mettler Toledo STARe SYSTEM TGA/DSC 3+.
DFT and TDDFT simulations have been performed with the Gaussian package (Gaussian09 revision D.01).[38] We used the B3LYP hybrid exchange-correlation functional, which, in combination with TDDFT, has been shown to reproduce very well the adsorption spectra of Ir-complexes.[39,40] We used the 6−31G(d,p) basis set for the light atoms and the aug−cc−pVDZ+ECP (Effective Core Potential) for iridium, which includes spin orbit at the scalar-relativistic level.[41] Thus, the effect of spin orbit on the valence states are not treated explicitly in our calculations. To obtain the optical absorption spectra up to 250−300 nm, we included 100 singlets and 100 triplets.
The triplet emission energies have been calculated with three different approaches, the first two based on the ΔSCF method, the third by TDDFT: (1) as the energy difference between T1 and the ground state S0, at their relaxed geometries. This is good approximation of the 0–0 emission peak at low temperature. (2) as the energy difference between the T1 and the S0 at the T1 relaxed geometry (vertical transition). (3) as the TDDFT vertical excitation at the T1 geometry in the Tamm−Dancoff approximation (TDA), to avoid the issues with the triplet instability.[42] We did not include solvent effects because, as reported in literature, they have a minor effect on the absorption/emission wavelengths for this class of dyes. We also did not calculate account vibrational progressions, but rather we have applied a gaussian broadening of 0.2 eV to the calculated transitions.

Conflicts of interest

There are no conflicts to declare.

Acknowledgements

We acknowledge the CINECA award under the ISCRA initiative (grant #HP10CJYU54), for the availability of high performance computing resources and support. For the financial support: Progetto Integrato Regione Lombardia and Fondazione CARIPLO (grant numbers 12689/13, 7959/13; Azione 1 e 2, “SmartMatLab centre” and Cariplo Foundation grant 2013-1766) and project "I-ZEB Verso Edifici Intelligenti a Energia Zero per la crescita della città intelligente" in the framework Accordo Quadro tra Regione Lombardia e Consiglio Nazionale delle Ricerche" July 17, 2015. for. The authors also acknowledge Dr. Mariacecilia Pasini and Dr. Silvia Destri of the CNR Institute for Macromolecular Studies (ISMAC) who provided the H*dtdk* ligand and Dr. Serena Cappelli of the Dept. of Chemistry of the University of Milan for the DSC/TGA analysis.

Notes and references

1 H. Yersin, Highly Efficient OLEDs with Phosphorescent Materials, Wiley-VCH, Weinheim, 2007.
2 E. Longhi and L. De Cola in *Iridium(III) in Optoelectronic and Photonics Applications*, ed. by Eli Zysman-Colman, John Wiley & Sons, Ltd, Chichester, 2017, chapter 6, pp. 205-273.
3 T. Hofbeck and H. Yersin, The triplet state of fac-Ir(ppy)$_3$, *Inorg. Chem.*, 2010, **49**, 9290–9299.
4 A. J. Huckaba and M. K. Nazeeruddin, Strategies for Tuning Emission Energy in Phosphorescent Ir(III) Complexes, *Comments Inorg. Chem.*, 2016, 1–29.
5 A. B. Tamayo, B. D. Alleyne, P. I. Djurovich, S. Lamansky, I. Tsyba, N. N. Ho, R. Bau and M. E. Thompson, Synthesis and

View Article Online
DOI: 10.1039/C8PP00052B

Characterization of Facial and Meridional Tris-cyclometalated Iridium(III) Complexes, *J. Am. Chem. Soc.*, 2003, **125**, 7377–7387.

6 A. Tsuboyama, H. Iwawaki, M. Furugori, T. Mukaide, J. Kamatani, S. Igawa, T. Moriyama, S. Miura, T. Takiguchi, S. Okada, M. Hoshino and K. Ueno, Homoleptic Cyclometalated Iridium Complexes with Highly Efficient Red Phosphorescence and Application to Organic Light- Emitting Diode, *J. Am. Chem. Soc.*, 2003, **125**, 12971–12979.

7 Z. Liu, D. Nie, Z. Bian, F. Chen, B. Lou, J. Bian and C. Huang, Photophysical Properties of Heteroleptic Iridium Complexes Containing Carbazole-Functionalized β-Diketonates, *Chem. Phys. Chem.*, 2008, **9**, 634–640.

8 S. Lamansky, P. Djurovich, D. Murphy, F. Abdel-Razzaq, H.-E. Lee, C. Adachi, P. E. Burrows, S. R. Forrest and M. E. Thompson, Highly Phosphorescent Bis-Cyclometalated Iridium Complexes: Synthesis, Photophysical Characterization, and Use in Organic Light Emitting Diodes, *J. Am. Chem. Soc.*, 2001, **123**, 4304–4312.

9 E. Baranoff and B. F. E. Curchod, FIrpic: archetypal blue phosphorescent emitter for electroluminescence, *Dalton Trans.*, 2015, **44**, 8318-8329.

10 Q. Zhao, L. Li, F. Li, M. Yu, Z. Liu, T. Yi and C. Huang, Aggregation-induced phosphorescent emission (AIPE) of iridium(III) complexes, *Chem. Commun.*, 2008, 685–687.

11 A. Poma, A. Forni, C. Baldoli, P. R. Mussini and A. Bossi, Cyclometalated Pt(II) complex with bidentate Schiff-base ligand displaying unexpected cis/trans isomery: synthesis, structures and electronic properties, *Dalton Trans*., 2017, **46**, 12500–12506.

12 J. Li, P. I. Djurovich, B. D. Alleyne, I. Tsyba, N. N. Ho, R. Bau and M. E. Thompson, Synthesis and characterization of cyclometalated Ir(III) complexes with pyrazolyl ancillary ligands, *Polyhedron*, 2004, **23**, 419–428.

13 K. Biennemans in *Handbook on the Physics and Chemistry of Rare Earths* Vol. 35, Ed. K.A. Gschneidner, Jr., J.-C.G. Bünzli and V.K. Pecharsky, 2005 Elsevier B.V ch.225.

14 Y. Suwa, M. Yamaji and H. Okamoto, Synthesis and photophysical properties of difluoroboronated β-diketones with the fluorene moiety that have high fluorescence quantum yields, *Tetrahedron Lett*., 2016, **57**, 1695–1698.

15 P. Z. Chen, L. Y. Niu, Y. Z. Chen and Q. Z. Yang, Difluoroboron β-diketonate dyes: Spectroscopic properties and applications, *Coord. Chem. Rev.*, 2017, **350**, 196-216.

16 E. Cognÿ-Laage, J.-F. Allemand, O. Ruel, J.-B. Baudin, V. Croquette, M. Blanchard-Desce and L. Jullien, Diaroyl(methanato) boron Difluoride Compounds as Medium-Sensitive Two-Photon Fluorescent Probes, *Chem. Eur. J.*, 2004, **10**, 1445–1455.

17 K. Ono, K. Yoshikawa, Y. Tsuji, H. Yamaguchi, R. Uozumi, M. Tomura, K. Taga and K. Saito, Synthesis and photoluminescence properties of BF_2 complexes with 1,3-diketone ligands, *Tetrahedron*, 2007, **63**, 9354-9358.

18 J. Li, P. I. Djurovich, B. D. Alleyne, M. Yousufuddin, N. N. Ho, J. C. Thomas, J. C. Peters, R. Bau and M. E. Thompson, Synthetic Control of Excited-State Properties in Cyclometalated Ir(III) Complexes Using Ancillary Ligands, *Inorg. Chem.*, 2005, **44**, 1713–1727.

19 S. Kesarkar, W. Mróz, M. Penconi, M. Pasini, S. Destri, M. Cazzaniga, D. Ceresoli, P. R. Mussini, C. Baldoli, U. Giovanella and A. Bossi, Near-IR Emitting Iridium(III) Complexes with Heteroaromatic β-Diketonate Ancillary Ligands for Efficient Solution-Processed OLEDs: Structure– Property Correlations, *Angew. Chem. Int. Ed.*, 2016, **55**, 2714–2718.

20 K.R.J. Thomas, M.Velusamy, J.T.Lin, C.H. Chien, Y.T. Tao, Y.S. Wen, Y.H. Hu and P. T. Chou, Efficient Red-Emitting Cyclometalated Iridium(III) Complexes Containing Lepidine-Based Ligands, *Inorg. Chem.*, 2005, **44**, 5677– 5685.

21 C. Dragonetti, L. Falciola, P. Mussini, S. Righetto, D. Roberto, R. Ugo and A. Valore, The Role of Substituents on Functionalized 1,10-Phenanthroline in Controlling the Emission Properties of Cationic Iridium(III) Complexes of Interest for Electroluminescent Devices, *Inorg. Chem.*, 2007, **46**, 8533-8547.

22 M. K. Nazeeruddin, R. Humphry-Baker, D. Berner, S. Rivier, L. Zuppiroli and M. Graetzel, Highly Phosphorescence Iridium Complexes and Their Application in Organic Light-Emitting Devices, *J. Am. Chem. Soc.*, 2003, **125**, 8790–8797.

23 K. Beydoun, M. Zaarour, J.A.G.Williams, T.Roisnel, V. Dorcet, A. Planchat, A.Boucekkine, D. Jacquemin, H. Doucet and V. Guerchais, Palladium-Catalyzed Direct Arylation of Luminescent Bis-Cyclometalated Iridium(III) Complexes Incorporating C^N- or O^O-Coordinating Thiophene-Based Ligands: an Efficient Method for Color Tuning, *Inorg. Chem.*, 2013, **52**, 12416–12428.

24 H. Ferreira, M. M. Conradie, K. G. von Eschwege, J. Conradie, Electrochemical and DFT study of the reduction of substituted phenanthrolines, *Polyhedron*, 2017, **122**, 147–154.

25 Md. S. Hossain, B. Muralidharan and K. H. Bevan, A General Theoretical Framework for Characterizing Solvated Electronic Structure via Voltammetry: Applied to Carbon Nanotubes, *J. Phys. Chem. C*, 2017, **121**, 18288-12298.

26 T. Tsuneda and K. Hirao, Self-interaction corrections in density functional theory, *J. Chem. Phys.*, 2014, **140**, 18A513.

27 M. Penconi, M. Cazzaniga, S. Kesarkar, P. R. Mussini, D. Ceresoli and A. Bossi, Upper limit to the ultimate achievable emission wavelength in near-IR emitting cyclometalated iridium complexes, *Photochem. Photobiol. Sci*., 2017, **16**, 1220-1229.

28 M. E. Thompson, P. I. Djurovich, S. Barlow and S.R.Marder in *Comprehensive Organometallic Chemistry*, ed. D. OÏHare, Vol. 12, Elsevier, Oxford, 2007, pp. 101-194.

29 A. Bossi, A. F. Rausch, M. Leitl, R. Czerwieniec, M. T. Whited, P. I. Djurovich, H. Yersin and M. E. Thompson, Photophysical Properties of Cyclometalated Pt(II) Complexes: Counterintuitive Blue Shift in Emission with an expanded ligand π-system, *Inorg. Chem.,* 2013, **52**, 12403-12415.

30 Q. Xin, W. L. Li, W. M. Su, T. L. Li, Z. S. Su, B. Chu and B. Li, Emission mechanism in organic light-emitting devices comprising a europium complex as emitter and an electron transporting material as host, *J. App. Phys.*, 2007, **101**, 044512.

31 C. Freund, W. Porzio, U. Giovanella, F. Vignali, M. Pasini, S. Destri, A. Mech, S. Di Pietro, L. Di Bari and P. Mineo, Thiophene Based Europium β-Diketonate Complexes: Effect of the Ligand Structure on the Emission Quantum Yield, *Inorg. Chem.,* 2011, **50**, 5417-5429.

32 R. A. Maya, A. Maity and T. S. Teets, Fluorination of Cyclometalated Iridium β-Ketoiminate and β-Diketiminate Complexes: Extreme Redox Tuning and Ligand-Centered Excited States, *Organometallics*, 2016, **35**, 2890–2899.

33 T.-T. Huang, T.-P. Chou, and E. Y. Li, Theoretical Characterizations on Charge Transfer Excitations in Solution by Time-Dependent Density Functional Theory A Case Study, *J. Chin. Chem. Soc.,* 2016, **63**, 465-471.

34 H. F. Higginbotham, C.-L. Yi, A. P. Monkman and K.-T. Wong, Effects of Ortho-Phenyl Substitution on the rISC Rate of D–A Type TADF Molecules, *J. Phys. Chem. C*, 2018, **122**, 7627-7634.

35 K. Sato, K. Shizu, K. Yoshimura, A. Kawada, H. Miyazaki and C. Adachi, Organic Luminescent Molecule with Energetically Equivalent Singlet and Triplet Excited States for Organic Light-Emitting Diodes, *Phys. Rev. Lett.*, 2013, **110**, 247401.

36 K. Dedeian, P.I. Djurovich, F.O. Garces, G. Carlson and R.J. Watts, A new synthetic route to the preparation of a series

View Article Online
DOI: 10.1039/C8PP00052B

of strong photoreducing agents: fac-tris-ortho-metalated complexes of iridium(III) with substituted 2-phenylpyridines, *Inorg. Chem*., 1991, **30**, 1685-1687.

37 S. Lamansky, P. Djurovich, D. Murphy, F. Abdel-Razaq, R. Kwong, I. Tsyba, M. Bortz, B. Mui, R. Bau and M.E. Thompson, Synthesis and Characterization of Phosphorescent Cyclometalated Iridium Complexes, *Inorg. Chem*., 2001, **40**, 1704-1711.

38 Gaussian 09, Revision D.01, M. J. Frisch, G. W. Trucks, H. B. Schlegel, G. E. Scuseria, M. A. Robb, J. R. Cheeseman, G. Scalmani, V. Barone, B. Mennucci, G. A. Petersson, H. Nakatsuji, M. Caricato, X. Li, H. P. Hratchian, A. F. Izmaylov, J. Bloino, G. Zheng, J. L. Sonnenberg, M. Hada, M. Ehara, K. Toyota, R. Fukuda, J. Hasegawa, M. Ishida, T. Nakajima, Y. Honda, O. Kitao, H. Nakai, T. Vreven, J. A. Montgomery, Jr., J. E. Peralta, F. Ogliaro, M. Bearpark, J. J. Heyd, E. Brothers, K. N. Kudin, V. N. Staroverov, T. Keith, R. Kobayashi, J. Normand, K. Raghavachari, A. Rendell, J. C. Burant, S. S. Iyengar, J. Tomasi, M. Cossi, N. Rega, J. M. Millam, M. Klene, J. E. Knox, J. B. Cross, V. Bakken, C. Adamo, J. Jaramillo, R. Gomperts, R. E. Stratmann, O. Yazyev, A. J. Austin, R. Cammi, C. Pomelli, J. W. Ochterski, R. L. Martin, K. Morokuma, V. G. Zakrzewski, G. A. Voth, P. Salvador, J. J. Dannenberg, S. Dapprich, A. D. Daniels, O. Farkas, J. B. Foresman, J. V. Ortiz, J. Cioslowski, and D. J. Fox, Gaussian, Inc., Wallingford CT, 2013.

39 S. Xu, J. Wang, H. Xia, F. Zhao and Y. Wang, Computational prediction for emission energy of iridium (III) complexes based on TDDFT calculations using exchange-correlation functionals containing various HF exchange percentages, *J. Mol. Model.*, 2015, **21**, 22.

40 C. Latouche, D. Skouteris, F. Palazzetti and V. Barone, TD-DFT Benchmark on Inorganic Pt(II) and Ir(III) Complexes, *J. Chem. Theory Comput.*, 2015, **11**, 3281−3289.

41 D. Figgen, K.A. Peterson, M. Dolg, and H. Stoll, Energy-consistent pseudopotentials and correlation consistent basis sets for the 5d elements Hf-Pt, *J. Chem. Phys.*, 2009, **130**, 164108.

42 M. J. G. Peach and D. J. Tozer, Excitation Energies from Time-Dependent Density Functional Theory for Linear Polyene Oligomers: Butadiene to Decapentaene, *J. Phys. Chem. A*, 2012, **116**, 9783−9789.

View Article Online
DOI: 10.1039/C8PP00052B

How the triplet energy of β-diketonate ancillary ligands in Ir(III) complexes affects the phosphorescence emission: photochemical and electrochemical investigations and DFT calculations shed light on the dark triplet excited states.

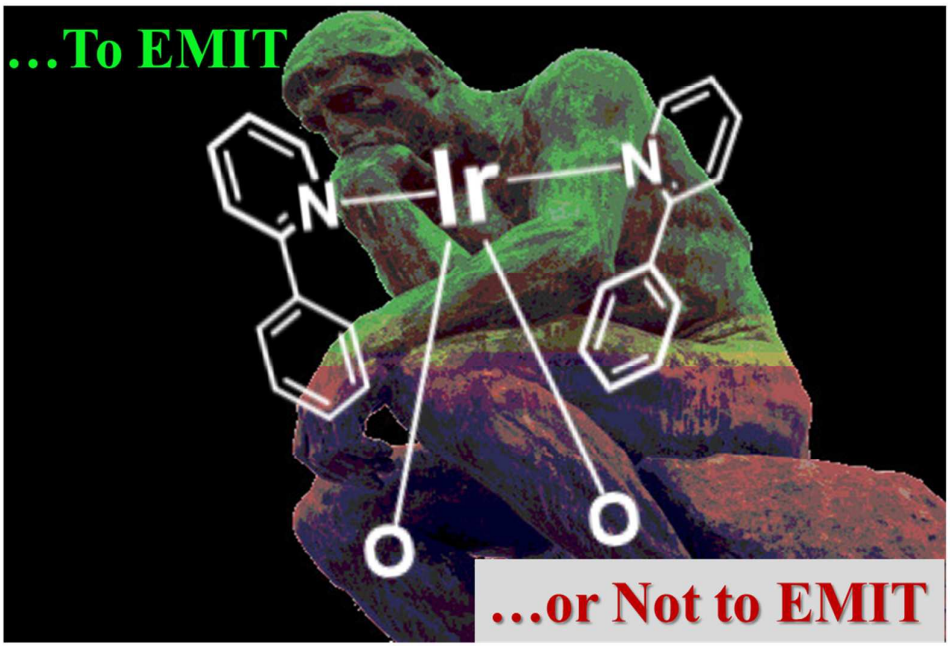

The thinker, Auguste Rodin